

CHAPTER – 2

**SIMULATION OF POWER SYSTEM
DYNAMICS**

2.1 Introduction :

Simulation of power system dynamics consists of setting up differential equations to represent the behaviour of dynamical variables of different components such as machines, controllers etc., and algebraic equations to relate the terminal quantities of these components with those of the network. In addition to this, for solving the above equations in digital computer, suitable numerical methods should be selected so that the computed response conforms acceptably with the actual response. Complexity of the model (number of differential-algebraic equations and number of parameters involved) depends on the nature of the problem and also on the required accuracy and the time length of response. For transient stability simulation studies it is sufficient to represent the transmission network behaviour by algebraic equations while the synchronous machines and the controllers need to be represented by their dynamic models with required degree of details. In the present work, simulation studies have been done using MATLAB by developing necessary program in MATLAB code. In the following sections, the models used for synchronous machine, the excitation system and the UPFC have been described.

2.2 Synchronous Machine Model :

The swing equation (2.1) alongwith the machine electrical power equation (2.3) gives the simplest model of synchronous machine known as the classical model. It represents the synchronous machine as a constant voltage behind a suitable reactance. Such a model, though simple, is insufficient for transient stability studies because it is not capable of taking into account the effects of the flux linkage variations of various machine circuits. Such variations have significant effects on the rotor dynamics. This necessitates machine representation in greater details, incorporating more dynamic variables and corresponding increase in the number of differential equations.

The state of the art of machine modelling is now such that synchronous machine transients can be modelled very accurately and comprehensively. Various machine models of different degrees of complexity are available in the literature, but all of them are either extension or simplification of the well known two-axes (d - q axes) model by R.H. Park [48]. A very accurate two-axes model by Jackson & Winchester[49] is available which is capable of including the effects of the important current carrying path in the solid iron rotor of the turbo-generators. But this model is too complex to allow its practical use in stability studies. A simpler model with seven rotor circuits (field, two d-axis damper and three q-axis damper) was derived from the previous model by Schultz, Jones & Ewart [50]. This model provides dynamic response equivalent to that produced by the Jackson-Winchester model, but this also is considered as unnecessarily complex for stability studies. The complexities of the above models are not only due to the increased computational burden arising from larger number of equations involved, but also due to the fact that many of the parameters used are nonstandard and their values are not easily available. The necessities of a machine model that gives reasonably accurate solution without requiring too much computational efforts, incited research in this direction. Comparative studies [51, 52] between different models have been reported. In these studies it has been observed that a model containing four rotor circuits, — field, one d-axis damper and two q-axis damper, apart from the d-axis and q-axis stator or armature circuits provide a very accurate model for the purpose of transient stability studies. This model is well capable of representing the subtransient and transient dynamics of d-axis as well as q-axis of both the salient-pole machines and the round rotor machines quite accurately. Moreover, it uses standard machine parameters [53, 54] which can be determined or measured from standard tests [55, 56]. In Park 's reference frame, the equations representing the flux dynamics of the above model can be written as :

Stator circuit equations :

$$\text{d - axis} \quad v_d = \dot{\psi}_d - \omega\psi_q - r_a i_d \quad (2.1a)$$

$$\text{q - axis} \quad v_q = \dot{\psi}_q + \omega\psi_d - r_a i_q \quad (2.1b)$$

Rotor circuit equations:

$$\text{field} \quad v_{fd} = \dot{\psi}_{fd} + r_{fd}i_{fd} \quad (2.1c)$$

$$\text{d - axis damper :} \quad 0 = \dot{\psi}_D + r_D i_D \quad (2.1d)$$

$$\text{q - axis damper 1 :} \quad 0 = \dot{\psi}_{Q1} + r_{Q1} i_{Q1} \quad (2.1e)$$

$$\text{q - axis damper 2 :} \quad 0 = \dot{\psi}_{Q2} + r_{Q2} i_{Q2} \quad (2.1f)$$

where ω = electrical angular speed (electrical radian/sec.)

and, with proper suffixes,

$$\left. \begin{array}{l} \Psi = \text{flux linkage} \\ i = \text{current} \\ r = \text{resistance} \\ v = \text{terminal voltage} \end{array} \right\} \text{ of respective circuits.}$$

In power system analysis, it is usually convenient to use a per unit (p.u.) system to normalize the variables. It is assumed that all the quantities in the above set of equations are in p.u. with respect to properly chosen base values. In the present work, the L_{ad} - base reciprocal p.u. system [57], the flux-linkage equations are given as follows :

Stator flux linkage equation :

$$\psi_d = -(L_{ad} + L_l)i_d + L_{ad}i_{fd} + L_{ad}i_D \quad (2.2a)$$

$$\psi_q = -(L_{aq} + L_l)i_q + L_{aq}i_{q1} + L_{aq}i_{Q2} \quad (2.2b)$$

Rotor flux equations :

$$\psi_{fd} = -L_{ffd}i_{fd} + L_{fD}i_D - L_{ad}i_d \quad (2.2c)$$

Note: The overhead dot will be used to denote time derivative throughout this text.

$$\psi_D = L_{fD}i_{fD} + L_{DD}i_D - L_{ad}i_d \quad (2.2d)$$

$$\psi_{Q1} = L_{Q11}i_{Q1} + L_{aq}i_{Q2} - L_{aq}i_q \quad (2.2e)$$

$$\psi_{Q2} = L_{Q22}i_{Q2} + L_{aq}i_{Q1} - L_{aq}i_q \quad (2.2f)$$

where

L_{ad} = mutual inductance between d-axis stator and d-axis rotor coils.

L_{aq} = mutual inductance between q- axis stator and q-axis rotor coils.

L_l = leakage inductance of the stator coils.

L_{ffd} = self inductance of the field coils.

L_{fd} = mutual inductance between field and d-axis damper.

L_{Q11} = self inductance of q-axis damper 1.

L_{Q22} = self inductance of q-axis damper 2.

Power developed by the machine is given by

$$P_e = v_d i_d + v_q i_q + (i_d^2 + i_q^2) r_a \quad (2.3a)$$

and the air-gap torque is given by

$$T_e = \psi_d i_q - \psi_q i_d \quad (2.3b)$$

Along with the above set of equations, the rotor swing equation

$$\frac{2H}{\omega_o} \ddot{\delta} = T_m - T_e \quad (2.4a)$$

where H is the p.u. inertia constant.

T_m is the mechanical input torque in p.u.

T_e is the air-gap torque in p.u.

ω_o is the rated(synchronous) speed in electrical radian/sec.

δ is the rotor angle in electrical radian measured with respect to synchronously rotating reference axis.

This gives an 8th order model of the overall synchronous machine. However, for stability studies, simplification of the stator voltage equations (2.1a) and (2.1b) is possible by neglecting

(i) the terms ψ_d and ψ_q .

(ii) the effect of speed variation on stator voltages.

The terms ψ_d and ψ_q represent the electrical transients in the stator circuits. Previous studies [58, 59] have shown that they have no appreciable effect on the electromechanical oscillations, and their removal from the stator voltage equation reduces appreciable amount of computational load without much affecting result.

Regarding (ii), the assumption normally taken is that $\omega = \omega_0 = 1$ p.u. in equations (2.1a) & (2.1b). This is, however, not meant that the speed is constant. It is simply assumed that the speed variation is small and do not have a significant effect on the voltages. In addition to the computational simplicity another advantage obtained through this assumption is that it counterbalances the effect of neglecting ψ_d and ψ_q on rotor electromechanical oscillations [47].

Due to the above two assumptions, the stator voltage equations reduce to the following algebraic equations :

$$v_d = -\psi_q - r_a i_d \quad (2.5a)$$

$$v_q = \psi_d - r_a i_q \quad (2.5b)$$

and result P_m and P_e in p.u. becomes equal to T_m and T_e in p.u. respectively, where P_m is the mechanical power input and P_e represents the electrical power output.

The swing equation (2.4a) can, therefore, be written as,

$$\frac{2H}{\omega_0} \ddot{\delta} = P_m - P_e \quad (2.6a)$$

However, to solve it in digital computer it is necessary to resolve the second order equation into two first order differential equations as given below:

$$\dot{\delta} = \omega \quad (2.6b)$$

$$\frac{2H}{\omega_o} \dot{\omega} = P_m - P_e \quad (2.6c)$$

Sometimes an additional damping term is added in the equation (2.6c) to take into account the damping effects provided by the damping windings and other factors. Equation (2.6c) in that case is modified as

$$\frac{2H}{\omega_o} \dot{\omega} = P_m - P_e - D(\omega - \omega_o) \quad (2.6d)$$

where D is called the damping coefficient.

As a result, the equations and terms relating the damper circuits can be omitted from the set of equations (2.1) and (2.2) and the reduced set of equations takes the following form:

Mechanical equation (swing equation):

$$\dot{\delta} = \omega \quad (2.7a)$$

$$\dot{\omega} = \frac{\omega_o}{2H} [P_m - P_e - D(\omega - \omega_o)] \quad (2.7b)$$

Electrical dynamics equation:

$$V_{fd} = \dot{\psi}_{fd} + r_{fd} i_{fd} \quad (2.7c)$$

Algebraic equations :

$$\psi_d = -(L_{ad} + L_1) i_d + L_{ad} i_{fd} \quad (2.7d)$$

$$\psi_q = -(L_{aq} + L_1) i_q \quad (2.7e)$$

$$\psi_{fd} = -L_{ffd} i_{fd} - L_{ad} i_d \quad (2.7f)$$

Hence, we have a 3rd order dynamic model of synchronous machines. It has been pointed out [46] that the above 3rd order model can produce machine response with acceptable accuracy in transient stability simulation studies.

In the literature, the machine dynamic equations are often written in terms of the more familiar variables and parameters such as transient and sub-transient voltages, reactances and the associated time constants. With proper conversion and manipulation of the set of equations (2.7a – 2.7f), following set of equations are obtained in terms of these new variables and parameters.

Mechanical equation:

$$\dot{\delta} = \omega \quad (2.8a)$$

$$\dot{\omega} = \frac{\omega_o}{2H} [P_m - P_e - D(\omega - \omega_o)] \quad (2.8b)$$

Electrical dynamics equation:

$$\dot{E}'_q = \frac{(E_f - E_q)}{T'_{do}} \quad (2.8c)$$

Algebraic equations:

$$E_q = E'_q + (x_d - x'_d)i_d \quad (2.8d)$$

$$v_d = -r_a i_d + x_q i_q \quad (2.8e)$$

$$v_q = E'_q - r_a i_q - x'_d i_d \quad (2.8f)$$

While the new variables and parameters are related with the old variables and parameters in the following way:

$$E'_q = \frac{L_{ad}}{L_{ffd}} \psi_{fd} = \text{voltage proportional to } \psi_{fd}$$

$$E_q = L_{ad} i_{fd} = \text{voltage proportional to } i_{fd}$$

$$E_f = \frac{L_{ad}}{r_{fd}} v_{fd} = \text{voltage proportional to } v_{fd}$$

and

$$x_d = \omega_o L_d = \omega_o (L_{ad} + L_l)$$

$$x_q = \omega_o L_q = \omega_o (L_{aq} + L_l)$$

$$x_d' = \omega_o L_d' = \omega_o (L_d - L_{ad}^2 / L_{ffd})$$

Where

E_d and E_q = machine internal voltages behind d - axis and q - axis synchronous reactances respectively.

E_q' = q - axis component of machine internal transient voltage.

x_d and x_q = d-axis and q - axis synchronous reactances respectively.

x_d' = d-axis transient reactances.

T_{do}' = d -axis open circuit transient time constant.

2.3 Model of Excitation System:

In the present study, the excitation system model shown in Fig.2.1 has been considered. It is representative of thyristor excitation system classified as type ST1A [60] excitation system. The model shown in Fig.2.1, however, has been simplified to include only those elements that are considered necessary for the present stability studies.

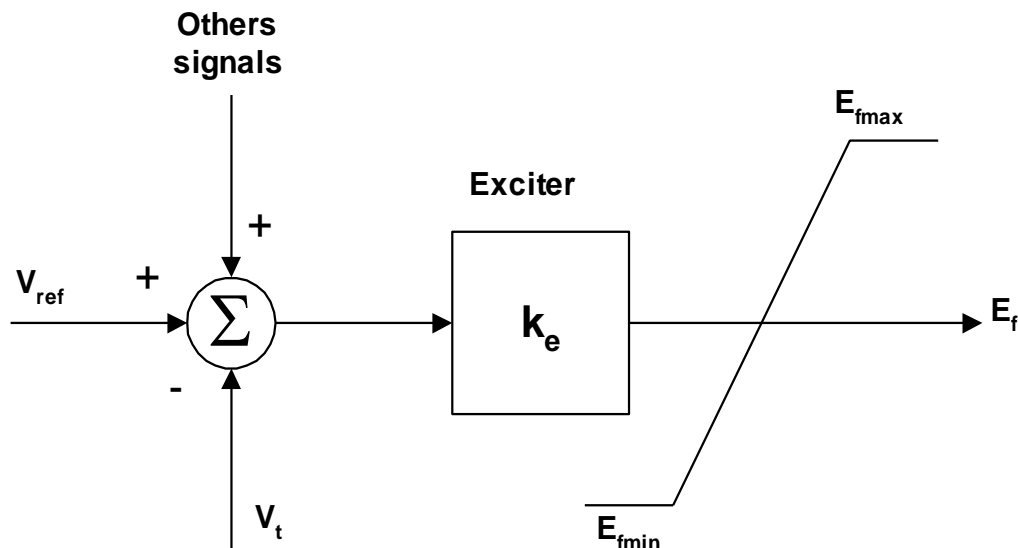


Fig.2.1: Excitation system IEEE-ST1A (Simplified)

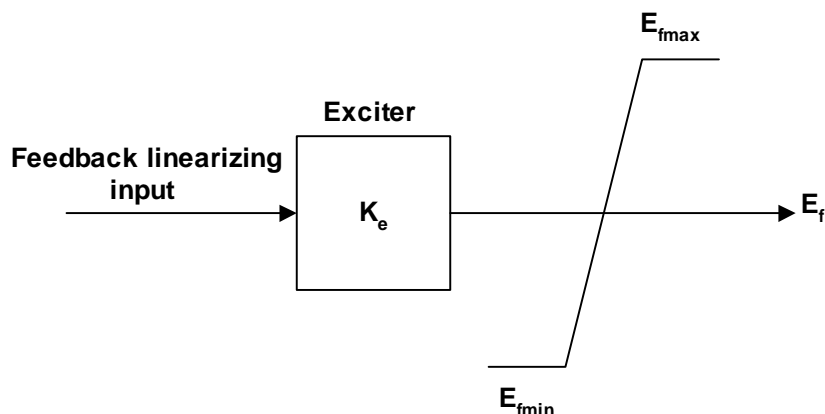


Fig.2.2: Excitation system as used in the present work

2.4 The Principle of UPFC Operation and Control:

A number of publications have appeared in the literature which describe the basic operating principles of the UPFC [8,9,14,15]. The schematic representation of the UPFC is shown in Fig.2.3. It consists of two back-to-back, self-commutated, voltage source converters, VSC-sh and VSC-se, using gate-turn-off (GTO) thyristors, sharing a shunt capacitor, C_{dc} , on a common d.c. link. One converter (VSC-sh) is coupled to the a.c.

system bus via a shunt transformer and the other (VSC-se) is coupled to the a.c. system via a series transformer. The magnitude and angle of the series injected voltage phasor, V_{se} determines the amount of power flow to be controlled. Assuming a loss-free converter operation, the UPFC as a whole neither absorbs nor injects active power with respect to the a.c. system. The active power, P_{se} , demanded by the series converter is supplied from the common d.c. link which, in turn, absorbs an equal amount of power, P_{sh} , from the a.c. system via the shunt converter to compensate the charge of the d.c. link capacitor C_{dc} and to keep the d.c. link voltage, V_{dc} , constant. So in the steady state, $P_{sh} + P_{se} = 0$, and V_{dc} remains constant. However, during transient, these constraints do not hold as there is a real power exchange between the d.c. capacitor and the a.c. system, and, consequently, V_{dc} varies. The d.c. link dynamics (i.e. the dynamics of the charging process of C_{dc}) then come into play in the process of power transfer. It is to be noted that unlike the active power, reactive power can be absorbed or generated by the converters independently.

The active and reactive power exchanged between the shunt converter and the a.c. system is controlled respectively by the phase angle and magnitude difference between the converter and the a.c. system bus voltages (i.e. \bar{V}_{sh} and \bar{V}_k). Accordingly V_{sh} and θ_{sh} (where $\bar{V}_{sh} = V_{sh} \angle \theta_{sh}$) determine the shunt reactive compensation while satisfying the constraints $P_{sh} + P_{se} = 0$, $V_k = \text{constant}$, and $V_{dc} = \text{constant}$. These two controllable variables are adjusted with respect to the reference signals V_{kref} and $V_{dc ref}$ respectively. The series converter controls the real and reactive power flow by varying the amplitude and angle of the series injected voltage \bar{V}_{se} . The controllable variables in this case, V_{se} and θ_{se} (where $\bar{V}_{se} = V_{se} \angle \theta_{se}$) are adjusted according to the reference signals Q_{mref} and P_{mref} , respectively.

In this work, pulse-width modulated (PWM) control [8,9] for the converter switching has been considered. With proper suffixes, m and θ denote the modulation ratio and phase angle of the PWM signals for the respective converters. The variables m and θ for respective converters are determined by the shunt and series control of the UPFC.

2.5 The UPFC model:

A number of steady state and dynamic models of UPFC have been proposed in the literature [24-29]. In essence, most of the suggested models have a common feature

that each of them represent the UPFC by an equivalent circuit consisting of two ideal voltage sources V_{sh} and V_{se} as shown in Fig.2.4, where Z_{sh} and Z_{se} are the impedances of the respective coupling transformers. Conventionally, for transient stability studies except for the synchronous machines and controllers, the electrical network is represented by its algebraic phasor equations. Thus the UPFC power circuit can be represented by the phasor equivalent of Fig.2.4. However, during transient, the dc capacitor of the UPFC exchanges energy with the system and consequently its voltage varies. Fast power flow control causes fluctuation of the dc link voltage. Hence, dynamics of the dc link voltage must be incorporated in the UPFC model for transient stability studies. Several UPFC models incorporating the dc link dynamics are available in the literature. In this work, the UPFC model suggested in [29] has been used. This model, shown in Fig.2.5 can represent the UPFC with fair degree of details including the d.c. link dynamics.

With the notations of Fig.2.5, one has:

$$P_k = P_{sh} + R_e \left\{ \overline{V}_k \cdot \overline{I}_m^* \right\} \quad (2.9a)$$

$$Q_k = Q_{sh} + I_m \left\{ \overline{V}_k \cdot \overline{I}_m^* \right\} \quad (2.9b)$$

$$P_m = -R_e \left\{ \overline{V}_k \cdot \overline{I}_m^* \right\} \quad (2.9c)$$

$$Q_m = -I_m \left\{ \overline{V}_k \cdot \overline{I}_m^* \right\} \quad (2.9d)$$

where $k_{sh} = \sqrt{(3/8)} m_{sh}$, m_{sh} is the modulation ratio of the shunt PWM controller .

The active power P_{sh} and the reactive power Q_{sh} absorbed by the shunt branch are given by:

$$P_{sh} = V_k^2 G_{sh} - K_{sh} V_{dc} V_k G_{sh} \cos(\theta_k - \theta_{sh}) - k_{sh} V_{dc} V_k B_{sh} \sin(\theta_k - \theta_{sh}) \quad (2.10a)$$

$$Q_{sh} = -V_k^2 B_{sh} + K_{sh} V_{dc} V_k B_{sh} \cos(\theta_k - \theta_{sh}) - k_{sh} V_{dc} V_k G_{sh} \sin(\theta_k - \theta_{sh}) \quad (2.10b)$$

where G_{sh} and B_{sh} are the conductance and susceptance of the shunt coupling transformer.

The current I_m and the voltage \overline{V} due to series compensation are:

$$\bar{i}_m = \left\{ \frac{(1 - \bar{a}_1)(\bar{V}_k - \bar{V}_m) - \bar{a}_2 \bar{V}_{se}}{(R_T + jX_T)} \right\} \quad (2.11a)$$

$$\bar{V} = \bar{a}_1(\bar{V}_k - \bar{V}_m) + \bar{a}_2 \bar{V}_{se} \quad (2.11b)$$

where,

$$V_{se} = k_{se} V_{dc} e^{j\theta_{se}} = \sqrt{\frac{3}{8}} m_{se} V_{dc} e^{j\theta_{se}} \quad (2.11c)$$

$$\bar{a}_1 = \frac{(R_{se} + jX_{se})}{\{(R_T - R_{se}) + j(X_T - X_{se})\}} \quad (2.11d)$$

$$\bar{a}_2 = \frac{(R_T - jX_T)}{\{(R_T - R_{se}) + j(X_T - X_{se})\}} \quad (2.11e)$$

In eqn. (2.11c), m_{se} is the modulation ratio of the series PWM controller, R_{se} and X_{se} are the resistance and reactance of the series coupling transformer, and R_T and X_T represent the resistance and reactance of the transmission line to which the UPFC is connected.

The dynamics of the d.c. circuit is described by the following differential equation:

$$\dot{V}_{dc} = \frac{P_{sh}}{CV_{dc}} + \frac{R_e \{\bar{V} \cdot \bar{i}_m^*\}}{CV_{dc}} - \frac{V_{dc}}{R_c C} - R_{sh} \frac{(P_{sh}^2 + Q_{sh}^2)}{CV_{dc} V_k^2} - \frac{R_{se} I_m^2}{CV_{dc}} \quad (2.12)$$

Note: Overhead bar has been used to denote phasor quantity throughout this text.

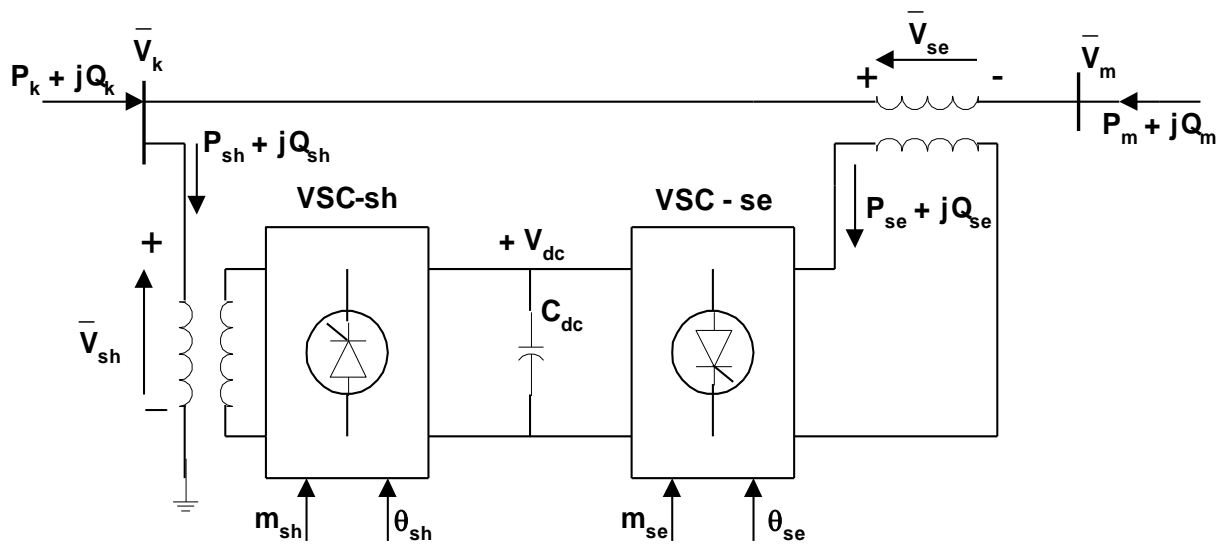


Fig. 2.3 Schematic diagram of UPFC

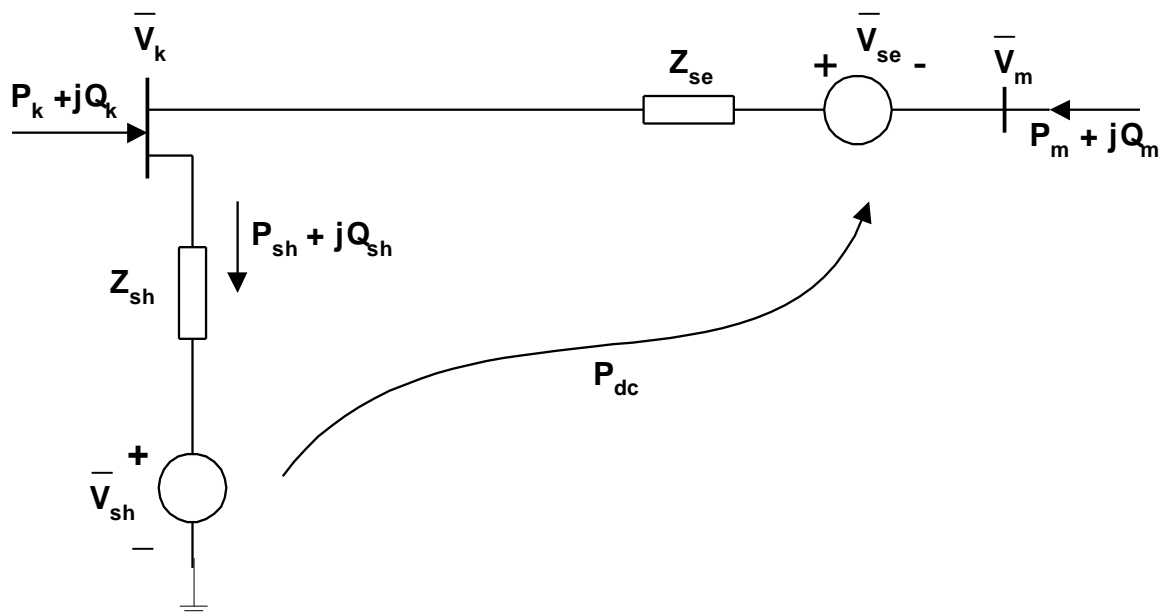


Fig. 2.4 Two voltage source equivalent circuit of UPFC

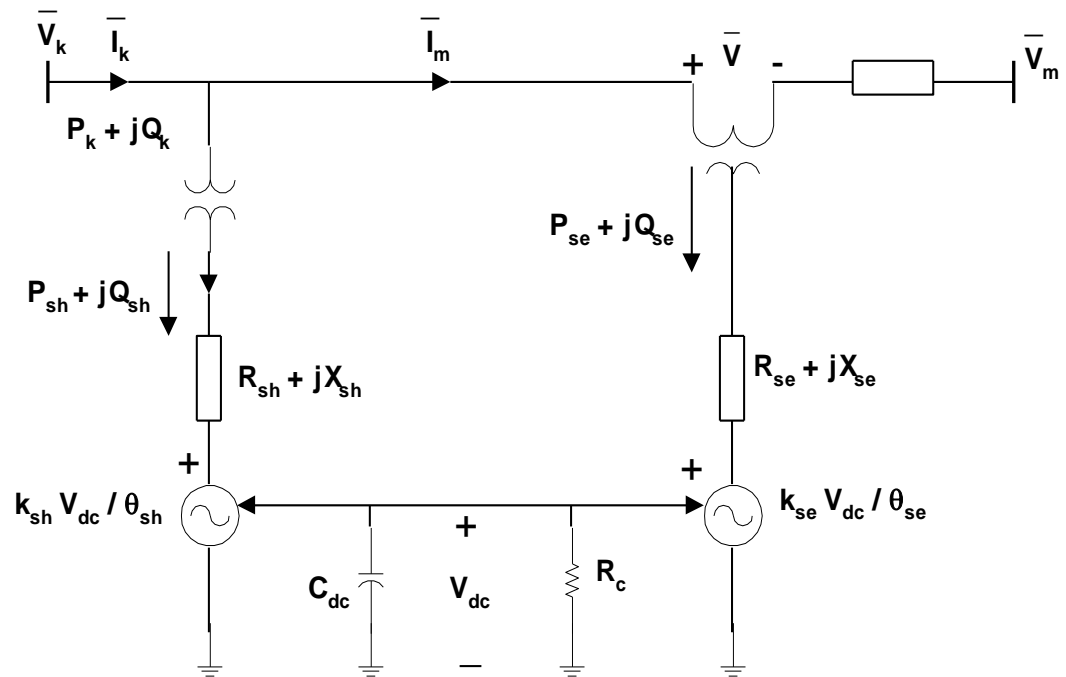


Fig.2.5 The UPFC model used in the Present Work

The models used for the shunt and series controllers are shown in Fig.2.6(a) and 2.6(b) respectively. However, in the simulation studies. The values of K_m 's are taken as '1', those for T_m 's are taken as '0' while K_p 's are taken as '0'. That is, effectively, integral controllers are used. Control is executed by adjusting the reference values of the integral controllers.

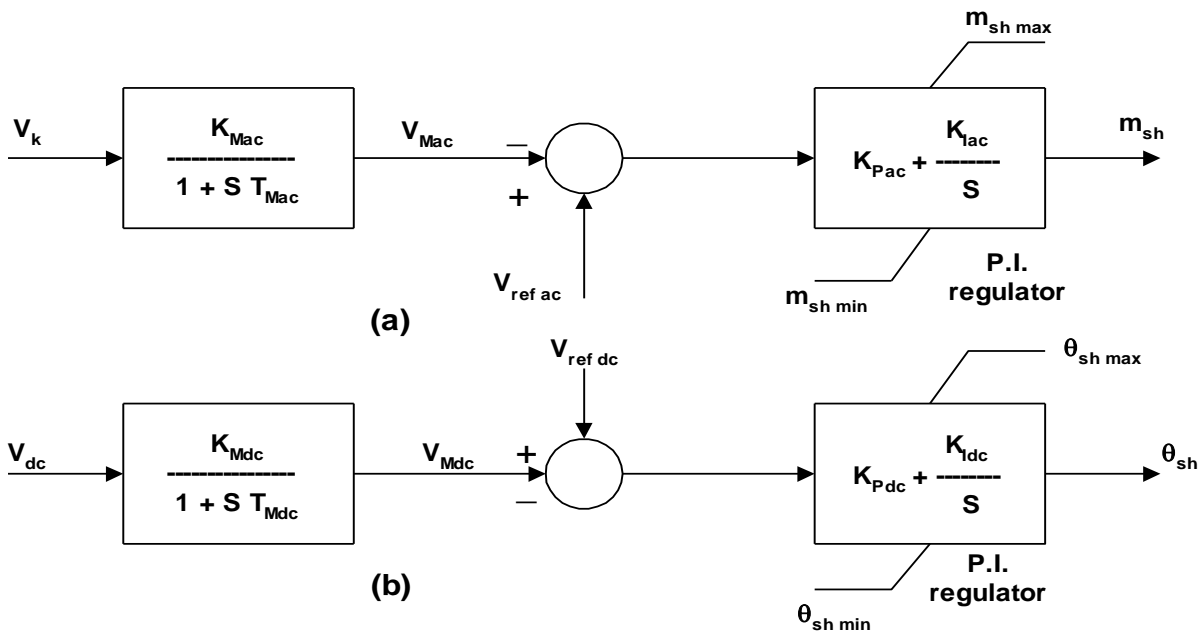


Fig. 2.6 UPFC shunt control block diagrams
(a) AC voltage control, (b) DC voltage control

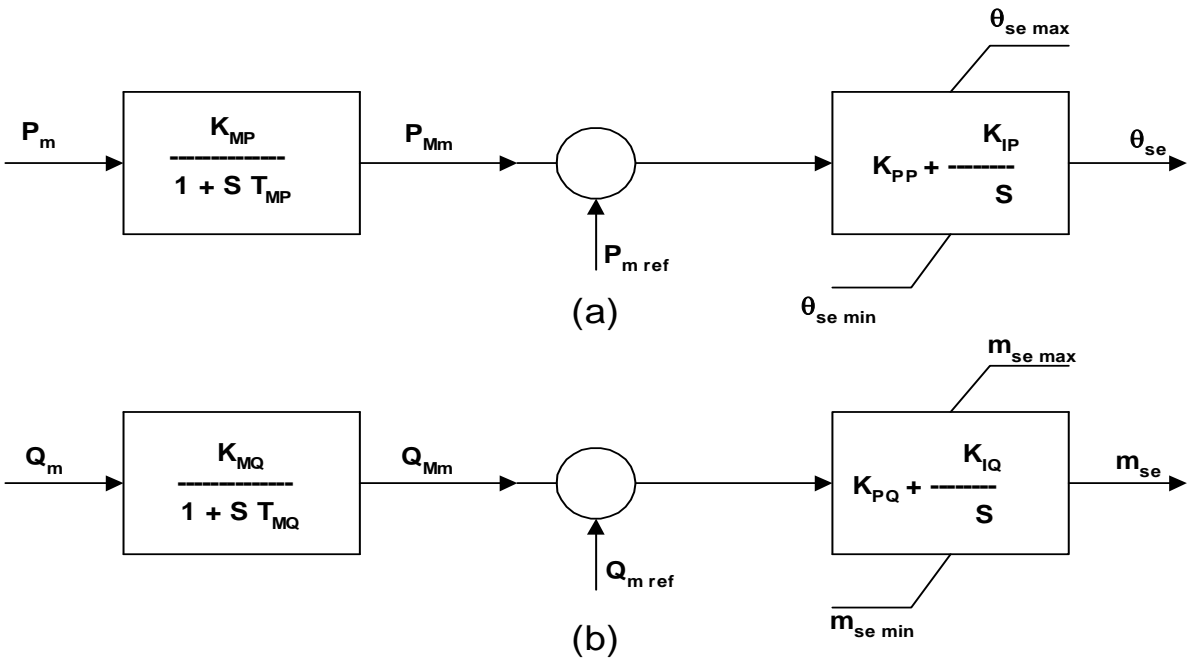


Fig.2.7 UPFC Series control block diagrams
(a) Active power control (b) Reactive power control